Available online at www.sciencedirect.com
ScienceDirect
Biochemical and Biophysical Research Communications 360 (2007) 219–225
BBRC
www.elsevier.com/locate/ybbrc

Human RON receptor tyrosine kinase induces complete epithelial-to-mesenchymal transition but causes cellular senescence

Marceline Côté [a], A. Dusty Miller [b], Shan-Lu Liu [a,*]

[a] *Department of Microbiology and Immunology, McGill University, Montreal, Canada*
[b] *Fred Hutchinson Cancer Research Center, Seattle, WA 98109, USA*

Received 6 June 2007
Available online 18 June 2007

Abstract

The RON receptor tyrosine kinase is a member of the MET proto-oncogene family and is important for cell proliferation, differentiation, and cancer development. Here, we created a series of Madin–Darby canine kidney (MDCK) epithelial cell clones that express different levels of RON, and have investigated their biological properties. While low levels of RON correlated with little morphological change in MDCK cells, high levels of RON expression constitutively led to morphological scattering or complete and stabilized epithelial-to-mesenchymal transition (EMT). Unexpectedly, MDCK clones expressing higher levels of RON exhibited retarded proliferation and senescence, despite increased motility and invasiveness. RON was constitutively tyrosine-phosphorylated in MDCK cells expressing high levels of RON and undergoing EMT, and the MAPK signaling pathway was activated. This study reveals for the first time that RON alone is sufficient to induce complete and stabilized EMT in MDCK cells, and overexpression of RON does not cause cell transformation but rather induces cell cycle arrest and senescence, leading to impaired cell proliferation.

Keywords: Recepteur d'origine Nantais (RON); Epithelial-to-mesenchymal transition (EMT); Cell proliferation; Cell migration and invasion; Senescence

The human RON (recepteur d'origine Nantais) receptor tyrosine kinase is a member of Met proto-oncogene family that includes mouse and cat Stk, and chicken Sea. The ligands for MET and RON/Stk were identified as hepatocyte growth factor (HGF) and macrophage stimulating factor (MSP), respectively. RON was originally identified in keratinocytes, and is expressed in a variety of human tissues, particularly those of epithelial origin. Overexpression of RON has been documented in a number of human cancer cell lines and tumors, and constitutively activated RON mutants have also been identified (reviewed by Wang et al. [1]). Further evidence pointing to a role of RON in tumorigenesis came from studies that overexpression of RON induces distal lung tumors in transgenic mice [2] and that constitutively activated RON mutants promote tumor metastasis and invasion [1], and malignant conversion in vivo [3].

One critical step towards the epithelial cancer is the loss of epithelial and gain of fibroblast characteristics, a process known as epithelial-to-mesenchymal transition (EMT). EMT is a highly conserved and fundamental process that also occurs during embryogenesis and wound healing [4]. It is characterized by the loss of epithelial markers, such as E-cadherin, and the gain of fibroblast markers, including α-smooth muscle actin. EMT has been extensively studied with the transforming growth factor β-1 (TGF-β1) and hepatocyte growth factor (HGF). Recently, MSP was also shown to induce partial EMT in RON-expressing MDCK cells, and TGF-β1 appeared to cooperate with MSP in this process [5].

Despite evidence supporting for the role of RON in tumorigenesis and metastasis in vivo, how human RON modulates cell growth, in particular, its transforming activity in vitro, remains controversial [6–8]. Here, we

* Corresponding author. Fax: +1 514 398 7052.
E-mail address: shan-lu.liu@mcgill.ca (S.-L. Liu).

0006-291X/$ - see front matter © 2007 Elsevier Inc. All rights reserved.
doi:10.1016/j.bbrc.2007.06.033

established a series of MDCK cell clones that express different levels of RON, and have investigated their biological properties. We demonstrate that the effects of RON in MDCK cells are actually more complex than previously described and are heavily dependent on the level of RON expression.

Materials and methods

Antibodies and reagents. Materials were purchased from the following suppliers: Anti-RON C20, Santa Cruz Biotechnology (Santa Cruz, CA); anti-phosphotyrosine 4G10, Upstate Biotechnology (Lake Placid, NY); BrdU, anti-α smooth muscle actin (α-SMA), anti-β-actin, and fluorescein isothiocyanate (FITC)-conjugated anti-mouse IgG, Sigma (St. Louis, MO); anti-BrdU, BD Biosciences (San Jose, CA); anti-E-cadherin, BD Transduction Laboratories (Mississauga, ON); anti-phospho-ERK, anti-ERK, anti-phospho-Akt, and anti-Akt, Cell Signaling Technology (Beverly, MA); horseradish peroxidase (HRP)-conjugated anti-mouse and anti-rabbit antibodies, Perkin-Elmer (Wellesley, MA); LY294002, PD98059, and Wortmannin, Calbiochem (San Diego, CA); MSP, R&D Systems (Minneapolis, MN). The monoclonal anti-RON antibody (ID1) was a kind gift from Immunotech (Marseille, France).

Immunoblotting and coimmunoprecipitation. Subconfluent cells were lysed, and cell lysates were subjected to 10% SDS–PAGE, followed by transfer to polyvinylidene difluoride (PVDF) membranes. Immunoblotting was performed as previously described [9]. To examine protein phosphorylation in the absence of growth factor stimulation, cells were incubated overnight in DMEM without serum before lysis.

Immunofluorescence. Immunostaining was performed as previously described [10] except that anti-E-cadherin (1:100) or anti-α-SMA (1:500) antibody was used. Pictures were taken using a Zeiss fluorescence microscope (Carl Zeiss, Germany).

Flow cytometry analysis. Cells were washed once with Hanks solution, and were detached by incubating with PBS plus 5 mM EDTA at 37 °C. The resuspended cells were washed twice with wash buffer (PBS containing 2% FBS), and 10^6 cells were incubated with an anti-RON monoclonal antibody ID1 for 2 h on ice. The cells were washed twice and then were incubated with FITC-conjugated anti-mouse IgG for 45 min, followed by staining with propidium iodide (2 μg/ml, Sigma) and FACScan analysis.

MTT assay. Cell growth was measured by MTT [3-(4,5-dimethylthiazol-2-yl)-2,5-diphenyltetrazolium bromide] assays following the manufacture's instructions (Sigma). Briefly, 5×10^3 cells per well were plated in 96-well plates in duplicate on day 0, and were assayed on days 1–6. For the assay, the cells were incubated with MTT for 2.5 h at 37 °C, followed by incubation with proper volumes of dimethyl sulfoxide (DMSO) and MTT solvent. The absorbance at 570 nm was then measured by an ELISA reader. The numbers of live cells were determined by standard curves generated for each cell line using different numbers of cells.

Migration assay. Cells (5×10^4/well) were grown on 24-well Transwell filters (Costar, Cambridge, MA) for 12 h, and were fixed using buffered formalin phosphate (Fisher Scientific, Ottawa, ON) for 20 min. Filters were washed three times with distilled water, and then stained with crystal violet for 20 min. After three washes with distilled water, nonmigrating cells were removed from the upper layer by using a cotton swab. The filters were then air-dried overnight, were photographed using a Zeiss microscope, and the migratory cells were quantified by measuring the pixels using a constant threshold for all images using the Scion Image software (Scion Corporation, Frederick, MD). Student's *t*-test was used for statistical analysis.

Invasion assay. Invasion assays were performed like the migration assays, except that the 24-well Transwell filters (Costar, Cambridge, MA) were pre-coated with Matrigel (100 μg/cm^2, BD Biosciences) before the cells were seeded and that the filters were stained and processed 36 h after the cells were seeded. Quantification of invading cells was performed as described for the migration assay.

β-Galactosidase (β-Gal) staining. β-Gal staining was performed as previously described by Dimri et al. [11] with minor modifications. Briefly, cells were washed once with PBS, fixed with 0.5% glutaraldehyde, and incubated with staining solution [1 mg/ml 5-bromo-4-chloro-3-indolyl β-D-galactoside (X-gal, Calbiochem), 0.12 mM potassium ferrocyanide, 0.12 mM potassium ferricyanide, 1 mM $MgCl_2$ in PBS at pH 6.0] overnight at 37 °C.

Cell cycle analysis. Cells were labeled with 10 μM BrdU (Sigma) for 3 h and were fixed with ice cold 70% ethanol for 30 min. Following a wash in washing buffer (PBS-0.5% BSA), cells were treated with 2 M HCl for 20 min, and resuspended in 0.1 M sodium borate pH 8.5 for 2 min at room temperature. Cells were washed and incubated with mouse anti-BrdU antibody for 30 min, followed by incubation with anti-mouse IgG coupled to FITC for 30 min at room temperature. Cells were treated with 5 μg/ml propidium iodide (PI) and 100 μg/ml RNaseA (Qiagen) in PBS for 30 min at 37 °C. Samples were analyzed by flow cytometry using Cell QUEST (BD Biosciences) and FlowJo software (FlowJo, LLC., Ashland, OR). Student's *t*-test was used for statistical analysis.

Results and discussion

Expression of human RON in MDCK cells results in morphological changes and RON tyrosine phosphorylation that depend on the level of RON expression

Overexpression of mouse Stk has been shown to induce morphological scattering and transformation in rodent fibroblasts [6,7]. However, the transforming activity of human RON appears to be lower than that of mouse Stk [6] and human Met [8]. This is also reflected in the RON-expressing RE7 cell line that shows no apparent morphological transformation [12]. Here, we established a series of MDCK clones, namely RON c1, c5, c6, and c8, which express various levels of human RON by transfection of MDCK cells with a retroviral vector [13] encoding the same human RON protein (Fig. 1A). Cell-surface expression of RON on these clones was determined by flow cytometry (Fig. 1B), and showed that c8 expressed the highest level of RON, followed in order by c5, c6, and c1. Notably, RE7 cells exhibited the lowest level of RON expression compared to these RON clones we generated (Fig. 1B).

The morphology of these MDCK/RON clones was examined. As shown in Fig. 1A, RON c5, c6, and c8 exhibited constitutive scattering, consistent with the relatively high levels of RON in these clones. RON c1 displayed a cobblestone-like epithelial morphology similar to the parental MDCK cells, also in parallel with its relatively low level of RON expression. RON c8 exhibited a somewhat flatter morphology than did RON c5 and c6, which we believe is due to severe senescence and cell cycle arrest induced by very high levels of RON expression in RON c8 (see details below).

We next determined if RON was tyrosine phosphorylated in these MDCK/RON clones. RON c5, c6, and c8 exhibited intense RON tyrosine phosphorylation (Fig. 1C), consistent with their higher levels of RON expression and scattered phenotypes. However, RON tyrosine phosphorylation was not detected in the parental

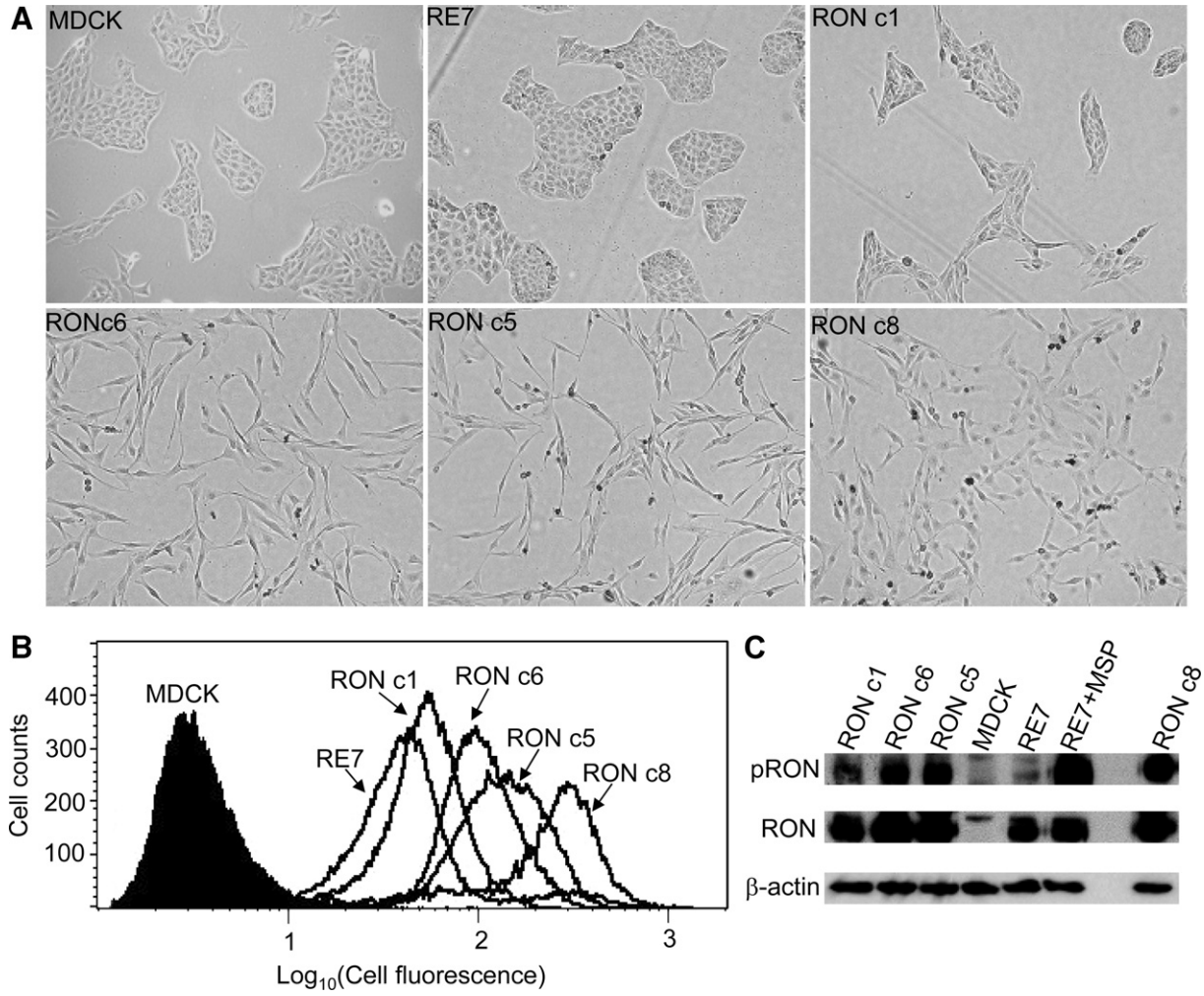

Fig. 1. RON induces morphological changes and tyrosine phosphorylations in MDCK cells in proportion to its expression level. (A) Morphology of MDCK clones expressing RON. Pictures were taken 2 days after equal numbers of cells from each cell line were seeded. (B) RON expression on the cell surface was examined by FACS. (C) RON tyrosine phosphorylation was detected by 4G10 antibody (upper). The membrane was then stripped and reprobed with anti-RON C20 (lower).

MDCK cells, and was barely detected in RON c1 and RE7 (Fig. 1C). Thus, RON was constitutively tyrosine phosphorylated in those MDCK clones expressing high levels of RON, and the extent of RON tyrosine phosphorylation largely correlated with the level of RON expression (Fig. 1B) and the degree of cell scattering (Fig. 1A).

RON activation leads to ERK/MAPK but not Akt phosphorylation. In general, RON tyrosine phosphorylation results in both ERK/MAPK and Akt activation. We therefore examined the status of ERK/MAPK and Akt phosphorylation in these MDCK cells expressing different levels of RON. ERK/MAPK was strongly phosphorylated in RON c5, c6, and c8 that expressed higher levels of RON, and treatment of cells with PD98059 essentially inhibited ERK/MAPK phosphorylation and partially reverted their scattered phenotype (Appendix Fig. 1). Surprisingly, however, Akt phosphorylation was not elevated in any of these RON-expressing MDCK clones (Appendix Fig. 1); instead, they exhibited basal or even reduced levels of phospho-Akt compared to that of the parental MDCK and RE7 cells (Appendix Fig. 1). The mechanism underlying the reduced Akt phosphorylation in these MDCK/RON clones is currently unclear, but may be associated with their impaired proliferation resulting from senescence and cell cycle arrest (see below). Importantly, MSP treatment of these clones enhanced their MAPK phosphorylation, and also markedly increased Akt phosphorylation (Appendix Fig. 1). These results strongly suggest that the mechanisms of RON activation by RON overexpression and by MSP stimulation are different in these RON-expressing MDCK cells. Noticeably, phosphorylation of ERK/MAPK but not Akt was also recently reported for the mouse Stk [14].

Complete EMT is associated with higher levels of RON expression

The loss of the epithelial cell marker E-cadherin and the gain of the fibroblast marker α-smooth muscle actin (α-SMA) are defined as the hallmarks of complete EMT [15]. To determine if the RON-induced scattering in

MDCK cells was typical of EMT, we first determined the expression of E-cadherin in the RON-expressing MDCK clones by immunostaining and immunoblotting. E-cadherin was abundantly expressed in the parental MDCK cells, as expected, and was detected at a somewhat reduced level in the flat RON c1 and in the RE7 cell lines (Fig. 2). In contrast, the E-cadherin expression was very low in RON c6, and was not detected in RON c5 (Fig. 2). Interestingly, E-cadherin expression was detected by immunoblotting in RON c8 (Fig. 2B), which could be related to its severe senescent phenotype induced by very high level RON expression.

Another critical feature that differentiates between reversible scattering and complete EMT of epithelial cells is the gain of the fibroblast marker, α-SMA [16]. Indeed, α-SMA was highly expressed in the scattered RON c5 and c6 (Fig. 2), and was also reproducibly detected at low levels in RON c8 by immunoblotting (Fig. 2B). In contrast, α-SMA was not detected in MDCK, RE7 or RON c1 (Fig. 2), consistent with their typical epithelial morphology. Thus, α-SMA was indeed expressed in the scattered MDCK cells that expressed relatively high levels of RON, indicating that these cells were undergoing EMT.

Collectively, our data indicate that expression of RON alone is sufficient to induce complete and stabilized EMT in MDCK cells that is independent of MSP or TGF-β1 stimulation, although a threshold level of RON expression is necessary for this process to occur. Our results are thus quite different from that of a previously published study by Wang et al. [5]. In that study, Wang et al reported partial EMT for RE7 cells by showing a diminished E-cadherin expression and spindled morphology of this cell line upon 10% FBS treatment. It is apparent from our current study that the RE7 cell line still expresses a substantial level of E-cadherin, albeit slightly lower compared to that of parental MDCK cells (Fig. 2). The discrepancies between our current study and the previously published report by Wang et al. might be due to experimental procedures used and/or the passage history of RE7 cells.

The molecular mechanisms underlying the development of EMT are still poorly understood. Notably, the Ras-Raf-MAPK and PI3K/Akt pathways have been shown to play important roles in this process [17]. We demonstrate here that ERK/MAPK is indeed extensively phosphorylated in the scattered RON c5, c6, and c8 undergoing EMT (Appendix Fig. 1), and MEK specific inhibitor, PD98059, rescues, at least partially, their EMT phenotypes and specific markers (data not shown). Interestingly, PI3K/Akt pathway was found not to be activated in these clones, as supported by the lack of Akt phosphorylation. Our results therefore support a role of ERK/MAPK, but not PI3K/Akt, in the RON-induced EMT in MDCK cells, which also agree with a previous study [5].

RON expression promotes cell motility and invasiveness

Given the complete EMT induced by RON, we next examined the motile activity and invasiveness of these MDCK/RON clones. RON c8 exhibited the highest motility and invasiveness among all the RON-expressing cells, as shown by its high intensity of crystal violet staining on the Transwell filters (Fig. 3A and C) and high average pixel counts measured by the Scion Image-NIH software (Fig. 3B and D). RON c5 and c6 cells were ~10-fold more motile ($p < 0.05$) and ~4-fold more invasive than RON c1 ($p < 0.05$), respectively (Fig. 3B and D). RE7 cells, by

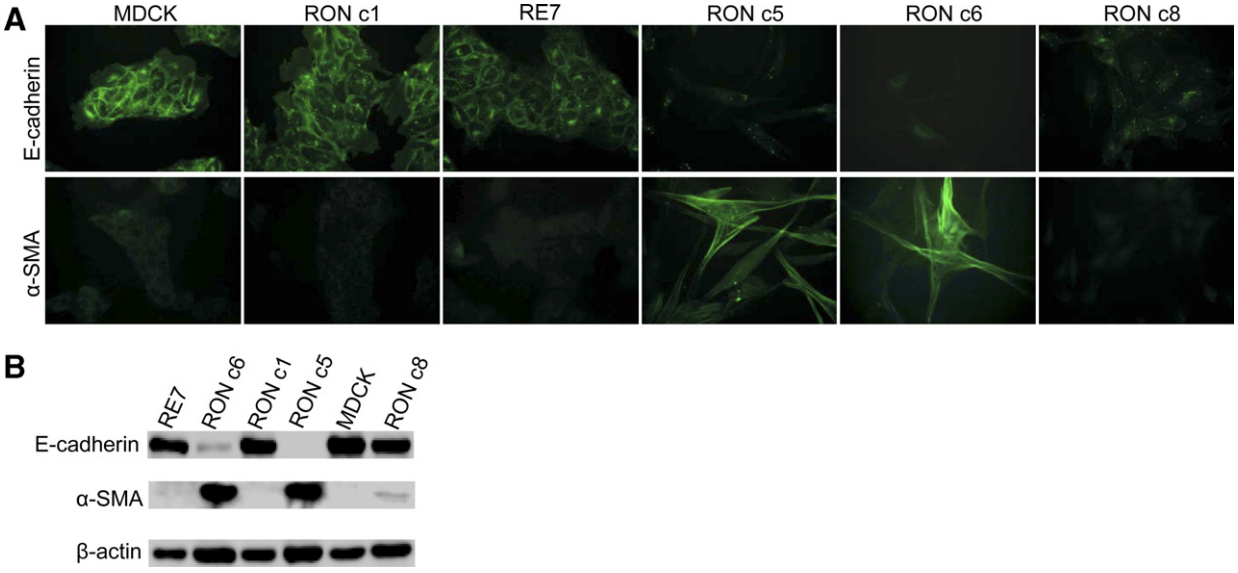

Fig. 2. Overexpression of RON in MDCK cells leads to complete EMT. (A) Immunostaining of E-cadherin and α-SMA in MDCK cells expressing RON. Cells were stained with a mouse anti-E-cadherin or anti-α-SMA antibody, followed by incubation with a FITC-conjugated goat anti-mouse IgG. The same conditions of illumination and photography were used in all panels. (B) Analyses of E-cadherin and α-SMA expression by immunoblotting.

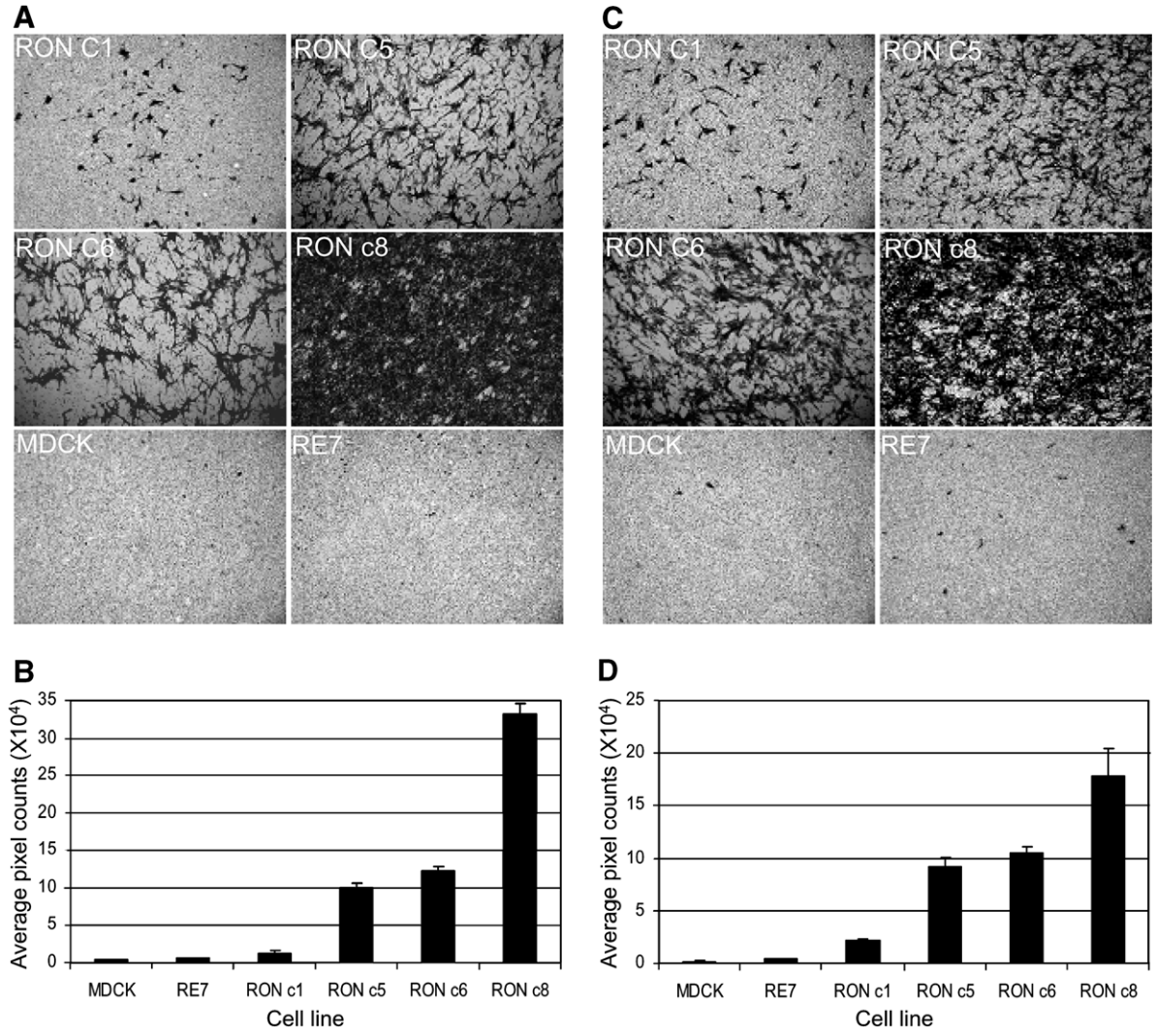

Fig. 3. MDCK cells expressing high levels of RON are constitutively motile (A and B) and invasive (C and D). See text for details. Pictures shown represent one of 3–4 independent experiments.

contrast, exhibited a background level of motility and invasiveness indistinguishable from that of parental MDCK cells ($p = 0.11$ and 0.30, respectively), consistent with the previous report that RE7 itself is not motile unless treated with MSP [18]. These results reveal that overexpression of human RON in MDCK cells inherently promotes cell motility and invasiveness, despite its inability to induce colony formation in the soft agar (Appendix Fig. 2). Moreover, the extent of cell motility and invasiveness correlated with the levels of RON expression and tyrosine phosphorylation, again suggesting that the RON kinase activation is involved in these processes.

High levels of RON expression in MDCK cells induce cell cycle arrest and senescence resulting in impaired cell proliferation

We next examined the growth kinetics of the RON-expressing cells using the MTT assay. As shown in Fig. 4A, RON c1 grew at a rate similar to that of parental MDCK cells, in accordance with their similarities in morphology and non-transformed nature. RON c5 and c8, however, showed markedly decreased rates of growth compared to those of RON c1 and the parental MDCK cells.

To determine if the retarded growth of RON c5 and c8 was due to slowed cell proliferation that may result from cell cycle arrest or senescence, we then performed cell cycle analysis in combination with the BrdU incorporation, and senescence-associated β-gal staining. RON c5 and c8 were found to be largely arrested in the G_0/G_1 phase, in comparison to the broader cell-cycle distribution of MDCK and RON c1 (Fig. 4B and C). BrdU staining indicated that RON c5 and c8 had significantly lower BrdU incorporation compared to that of MDCK and RONc1 (~5% for RON c5 and c8 vs. ~45% for MDCK and RON c1, $p < 0.05$) (Fig. 4B and C). β-gal staining at pH 6.0, a method that specifically detects senescence [11], indicated that RON c5 and c8 were undergoing senescence, in contrast to that of parental MDCK and RON c1 (Fig. 4D). Same sets of experiments were also performed on RON c6 with results

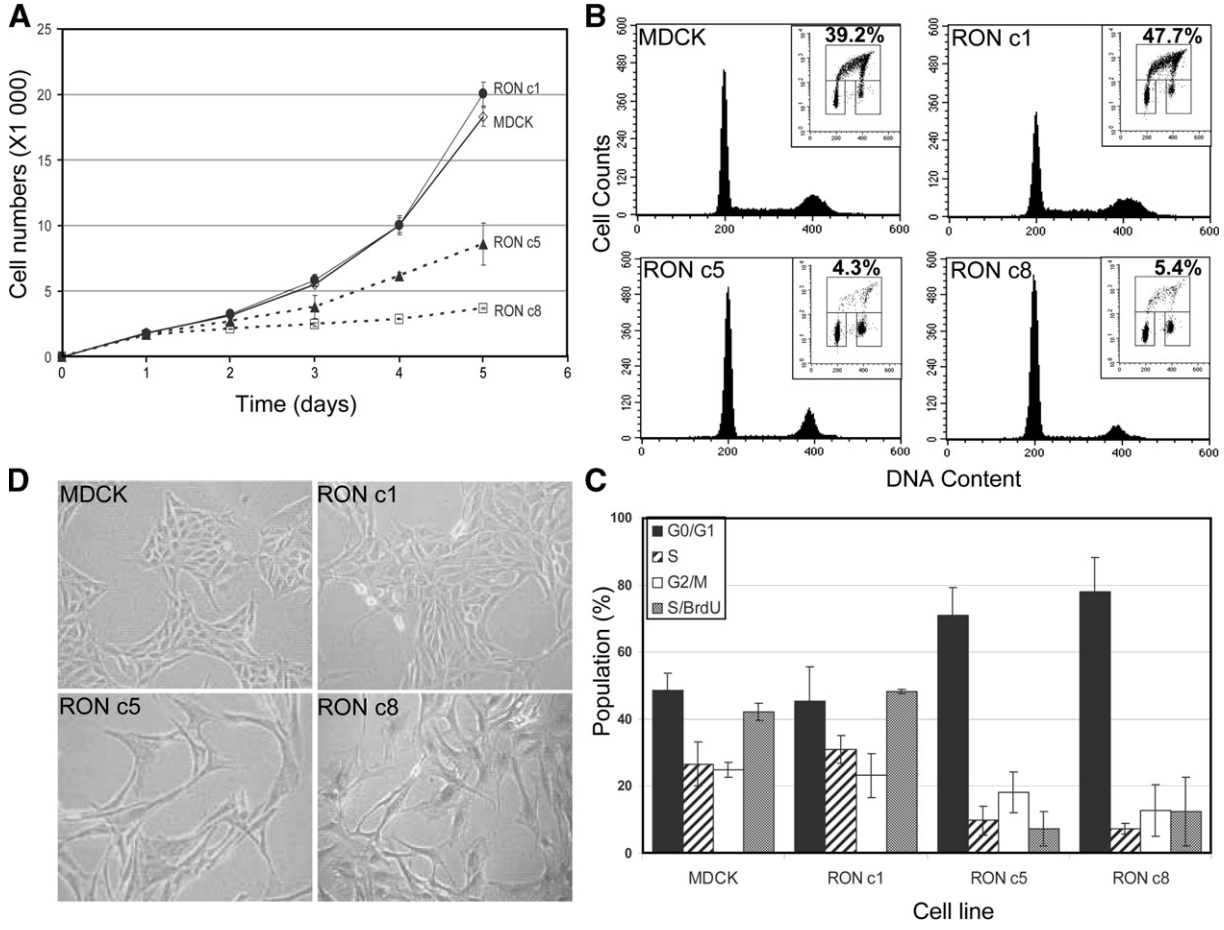

Fig. 4. High levels of RON expression in MDCK cells result in impaired cell proliferation, cell cycle arrest, and senescence. (A) MTT assays. Equal numbers of cells were plated onto 96-well plates in duplicate on day 0, and the cell viability was measured by MTT assays on day 1 through day 5. The values are the means of two independent experiments. (B) Cell cycle analysis. Subconfluent cultures were labeled with BrdU, stained with PI and analyzed by flow cytometry. Representative histograms display the DNA-content stained by PI (*X*-axis). (Insets) The upper-box represents the BrdU incorporation in S phase (*Y*-axis) with the DNA content shown on the *X*-axis. The numbers represent the percentages of BrdU-positive cells that were obtained from one representative experiment. The lower-left box displays the G_0/G_1 cell population, and the lower-right box displays the G_2/M cell population. (C) Summary of cell populations in G_1/G_0, S and G_2/M phases, as well as the BrdU incorporations in S phase. Data were obtained from 2 to 4 independent experiments. (D) β-Gal staining. Cells were seeded on day 0, and were stained on day 1 by β-gal at pH 6.0, and were photographed. Representative results from two independent experiments are shown. The same sets of experiments were also performed with MDCK/RON c6, with results similar to those for MDCK/RON c5.

similar to that of RON c5 (data not shown). Collectively, these data indicate that high level RON expression induces cell cycle arrest and senescence in MDCK cells, resulting in significantly impaired cell proliferation and growth. These results explained, at least in part, why none of these RON clones formed colonies in soft agar (Appendix Fig. 2).

Oncogene-induced cell death and senescence has been previously documented for several oncoproteins, prominently Myc and Ras, and is regarded as an important cellular failsafe program that counteracts cancer development [19]. Here, we demonstrate that high-level of RON expression in MDCK cells induces senescence and cell cycle arrest, resulting in impaired cell proliferation (Fig. 4), despite its ability to induce complete and stabilized EMT (Fig. 2).To our knowledge, this is the first report showing that overexpression of RON can inhibit cell proliferation and induce senescence.

The possible dual effect of RON on cell growth is reminiscent of the Ras oncoprotein, which has been shown to promote oncogenic transformation on one hand [20] but to induce premature senescence on the other [21]. Importantly, the dual effect of Ras on cell proliferation is cell-type [22] and cell-stage dependent [23], as well as relies on the levels of Ras expression and the intensity of its signaling [24]. For example, moderate expression of Ras in primary human fibroblasts results in increased proliferation, whereas overexpression of Ras in the same cell type leads to severe senescence [24]. In this sense, it will be interesting to determine if RON can impose distinct and even opposing effects in epithelial cells, especially primary epithelial cells. Noticeably, MSP has been previously shown to have dual effects in different RON-expressing cells, i.e., it induces apoptotic cell death in the mouse erythroleukemia cells but promotes proliferation in Ba/F3 pro-B cells [25].

The mechanism that underlies the RON-induced growth arrest and senescence remains to be better understood. We found that ERK/MAPK was strongly phosphorylated in cells expressing high levels of RON that exhibited significantly impaired proliferation and severe senescence, suggesting this pathway might play a critical role in this process. One possible scenario is that RON activates the Ras-Raf-MAPK signaling pathway that further feeds into the downstream p53-p21$^{WAF/CIP}$ and p16 signaling network, leading to senescence [21,26]. Additionally, the c-JNK and p38 pathways might be involved, which has been shown for the Ras-induced senescence in 293 cells [24] and the MSP-induced apoptosis in the mouse erythroleukemia cells expressing RON [25]. Experiments are in progress to examine these possibilities in order to better understand the mechanisms of RON-induced senescence in the MDCK cells.

Acknowledgments

We thank Morag Park for helpful discussions and critical reading of this manuscript. This work was supported by funds from the Canadian Institutes of Health Research and McGill University to S.-L. Liu, and grants from the US National Institutes of Health to A.D. Miller. Marceline Côté was supported by a scholarship from the Natural Sciences and Engineering Research Council of Canada. S.-L. Liu is a Canada Research Chair in Virology and Gene Therapy.

Appendix A. Supplementary data

Supplementary data associated with this article can be found, in the online version, at doi:10.1016/j.bbrc.2007.06.033.

References

[1] M.H. Wang, D. Wang, Y.Q. Chen, Oncogenic and invasive potentials of human macrophage-stimulating protein receptor, the RON receptor tyrosine kinase, Carcinogenesis 24 (2003) 1291–1300.
[2] Y.Q. Chen, Y.Q. Zhou, L.H. Fu, D. Wang, M.H. Wang, Multiple pulmonary adenomas in the lung of transgenic mice overexpressing the RON receptor tyrosine kinase. Recepteur d'origine nantais, Carcinogenesis 23 (2002) 1811–1819.
[3] E.L. Chan, B.E. Peace, M.H. Collins, K. Toney-Earley, S.E. Waltz, Ron tyrosine kinase receptor regulates papilloma growth and malignant conversion in a murine model of skin carcinogenesis, Oncogene 24 (2005) 479–488.
[4] J.P. Thiery, Epithelial–mesenchymal transitions in development and pathologies, Curr. Opin. Cell Biol. 15 (2003) 740–746.
[5] D. Wang, Q. Shen, Y.Q. Chen, M.H. Wang, Collaborative activities of macrophage-stimulating protein and transforming growth factor-beta1 in induction of epithelial to mesenchymal transition: roles of the RON receptor tyrosine kinase, Oncogene 23 (2004) 1668–1680.
[6] A.D. Miller, N.S. Van Hoeven, S.-L. Liu, Transformation and scattering activities of the receptor tyrosine kinase RON/Stk in rodent fibroblasts and lack of regulation by the jaagsiekte sheep retrovirus receptor, Hyal2, BMC Cancer 4 (2004) 64.
[7] B.E. Peace, M.J. Hughes, S.J. Degen, S.E. Waltz, Point mutations and overexpression of Ron induce transformation, tumor formation, and metastasis, Oncogene 20 (2001) 6142–6151.
[8] M.M. Santoro, C. Collesi, S. Grisendi, G. Gaudino, P.M. Comoglio, Constitutive activation of the RON gene promotes invasive growth but not transformation, Mol. Cell Biol. 16 (1996) 7072–7083.
[9] S.-L. Liu, M.I. Lerman, A.D. Miller, Putative phosphatidylinositol 3-Kianse (PI3K) binding motifs in ovine betaretrovirus Env proteins are not essential for rodent fibroblast transformation and PI3K/Akt activation, J. Virol. 77 (2003) 7924–7935.
[10] S.-L. Liu, F.M. Duh, M.I. Lerman, A.D. Miller, Role of virus receptor Hyal2 in oncogenic transformation of rodent fibroblasts by sheep betaretrovirus env proteins, J. Virol. 77 (2003) 2850–2858.
[11] G.P. Dimri, X. Lee, G. Basile, M. Acosta, G. Scott, C. Roskelley, E.E. Medrano, M. Linskens, I. Rubelj, O. Pereira-Smith, et al., A biomarker that identifies senescent human cells in culture and in aging skin in vivo, Proc. Natl. Acad. Sci. USA 92 (1995) 9363–9367.
[12] M.H. Wang, C. Ronsin, M.C. Gesnel, L. Coupey, A. Skeel, E.J. Leonard, R. Breathnach, Identification of the ron gene product as the receptor for the human macrophage stimulating protein, Science 266 (1994) 117–119.
[13] A. Danilkovitch-Miagkova, F.M. Duh, I. Kuzmin, D. Angeloni, S.-L. Liu, A.D. Miller, M.I. Lerman, Hyaluronidase 2 negatively regulates RON receptor tyrosine kinase and mediates transformation of epithelial cells by jaagsiekte sheep retrovirus, Proc. Natl. Acad. Sci. USA 100 (2003) 4580–4585.
[14] X. Wei, S. Ni, P.H. Correll, Uncoupling ligand-dependent and -independent mechanisms for mitogen-activated protein kinase activation by the murine Ron receptor tyrosine kinase, J. Biol. Chem. 280 (2005) 35098–35107.
[15] J.P. Thiery, Epithelial–mesenchymal transitions in tumour progression, Nat. Rev. Cancer 2 (2002) 442–454.
[16] J. Gotzmann, M. Mikula, A. Eger, R. Schulte-Hermann, R. Foisner, H. Beug, W. Mikulits, Molecular aspects of epithelial cell plasticity: implications for local tumor invasion and metastasis, Mutat. Res. 566 (2004) 9–20.
[17] S. Grunert, M. Jechlinger, H. Beug, Diverse cellular and molecular mechanisms contribute to epithelial plasticity and metastasis, Nat. Rev. Mol. Cell Biol. 4 (2003) 657–665.
[18] M.H. Wang, G.W. Cox, T. Yoshimura, L.A. Sheffler, A. Skeel, E.J. Leonard, Macrophage-stimulating protein inhibits induction of nitric oxide production by endotoxin- or cytokine-stimulated mouse macrophages, J. Biol. Chem. 269 (1994) 14027–14031.
[19] C.A. Schmitt, Senescence, apoptosis and therapy–cutting the lifelines of cancer, Nat. Rev. Cancer 3 (2003) 286–295.
[20] R.A. Weinberg, Oncogenes, antioncogenes, and the molecular bases of multistep carcinogenesis, Cancer Res. 49 (1989) 3713–3721.
[21] M. Serrano, A.W. Lin, M.E. McCurrach, D. Beach, S.W. Lowe, Oncogenic ras provokes premature cell senescence associated with accumulation of p53 and p16INK4a, Cell 88 (1997) 593–602.
[22] C. Guerra, N. Mijimolle, A. Dhawahir, P. Dubus, M. Barradas, M. Serrano, V. Campuzano, M. Barbacid, Tumor induction by an endogenous K-ras oncogene is highly dependent on cellular context, Cancer Cell 4 (2003) 111–120.
[23] J.A. Benanti, D.A. Galloway, The normal response to RAS: senescence or transformation? Cell Cycle 3 (2004) 715–717.
[24] Q. Deng, R. Liao, B.L. Wu, P. Sun, High intensity ras signaling induces premature senescence by activating p38 pathway in primary human fibroblasts, J. Biol. Chem. 279 (2004) 1050–1059.
[25] A. Iwama, N. Yamaguchi, T. Suda, STK/RON receptor tyrosine kinase mediates both apoptotic and growth signals via the multifunctional docking site conserved among the HGF receptor family, EMBO J. 15 (1996) 5866–5875.
[26] A.W. Lin, M. Barradas, J.C. Stone, L. van Aelst, M. Serrano, S.W. Lowe, Premature senescence involving p53 and p16 is activated in response to constitutive MEK/MAPK mitogenic signaling, Genes Dev. 12 (1998) 3008–3019.